f Electron Contribution to the Change of Electronic Structure in $CeRu_2Si_2$ with Temperature: A Compton Scattering Study

A. Koizumi,[1] G. Motoyama,[1] Y. Kubo,[2] T. Tanaka,[2] M. Itou,[3] and Y. Sakurai[3]

[1]*Graduate School of Material Science, University of Hyogo, Hyogo 678-1297, Japan*
[2]*Department of Physics, College of Humanities and Science, Nihon University, Tokyo 156-8550, Japan*
[3]*Japan Synchrotron Radiation Research Institute (JASRI), SPring-8, Hyogo 679-5198, Japan*

(Received 22 September 2010; published 28 March 2011)

High resolution Compton profiles have been measured in the single crystal of $CeRu_2Si_2$ above and below the Kondo temperature to elucidate the change of the Ce-4f electron from localized to itinerant states. Two-dimensional electron occupation number densities projected on the first Brillouin zone, which are obtained after a series of analyses, clearly specify the difference between itinerant and localized states. The contribution of Ce-4f electrons to the electronic structure is discussed by contrast with a band calculation.

DOI: 10.1103/PhysRevLett.106.136401 PACS numbers: 71.27.+a, 75.10.Lp, 78.70.Ck

The heavy fermion system shows a variety of interesting properties since a strongly correlated f electron changes its aspects depending on conditions such as temperature, magnetic field, pressure, and chemical substitution. The relative strength of the Kondo effect on the Ruderman-Kittel-Kasuya-Yosida interaction determines whether the underlying f electronic state is dominated by itinerant or localized characters. The studies of the f electronic state have so far ranged over many heavy fermion materials. Particularly, $CeRu_2Si_2$ is still an intriguing substance as a typical heavy fermion compound. According to the well-known Doniach phase diagram, $CeRu_2Si_2$ is considered to lie in the region where the Kondo effect is dominant over the Ruderman-Kittel-Kasuya-Yosida interaction. The Ce-4f electron hybridizes with a conduction electron below the Kondo temperature, T_K, and acquires the itinerant character as a heavy quasiparticle, while above T_K, the Ce-4f electron localizes in the paramagnetic state. The similar tendency is caused not just by temperature changes but also by magnetic field effect. Applying external field to $CeRu_2Si_2$ induces a metamagnetic transition around the field of $H_m \sim 7.7$ T at low temperature [1]. Above H_m, the Ce-4f electron localizes with induced magnetization. The substitution of Ge for Si, which brings negative chemical pressure upon a sample, transforms the system from nonmagnetic to antiferromagnetic or ferromagnetic states, and consequently the Ce-4f electron changes from itinerant to localized ones [2,3]. Hence, the substituted compounds are considered as an ideal system to study the quantum critical phenomenon depending on the chemical pressure [4,5]. In addition, since $CeRu_2Si_2$ has the same type of crystal structure as URu_2Si_2, which has an open issue so-called hidden order, it is really useful to know about the electronic state of $CeRu_2Si_2$ for comparison [6–9]. As just described, $CeRu_2Si_2$ is a key substance in understanding the electronic state of a heavy fermion system.

Actually, the electronic structure of $CeRu_2Si_2$ has been frequently investigated by using several experimental techniques. The de Haas–van Alphen (dHvA) studies reported the change in Fermi surface (FS) associated with the metamagnetic transition [3,10–14]. The dHvA signals have been often explained as compared with the FS topology derived from a band calculation [15–19]. When we simply look at the results, the Ce-4f electron seems to turn from itinerant to localized states across H_m. However, recent theoretical study has argued that the electronic state above H_m should be interpreted as a completely filled band rather than the localized state used in the customary sense [20]. Additionally, since the dHvA experiment requires lowering the temperature and applying strong magnetic fields to the sample, it is not clear whether or not the electronic state above H_m is similar to the localized state above T_K. The angle-resolved photoelectron spectroscopy (ARPES) experiment is also an effective method to investigate the electronic structure. Recent ARPES experiments reported the detailed band structure and FS of $CeRu_2Si_2$ [5,8,21]. In these studies, however, measurements were performed in the vicinity of T_K and temperature dependence has not been measured. The electronic structure of $CeRu_2Si_2$ was therefore discussed by contrast with that of related compounds such as $LaRu_2Si_2$ and $CeRu_2(Si_{1-x}Ge_x)_2$. Seen in this light, the difference of electronic structure in $CeRu_2Si_2$ between, above, and below T_K is still not revealed directly by using the same measurement in the same sample.

In this study, we have employed high resolution Compton profile (HRCP) measurement as another approach to investigate the change of Ce-4f electronic state in $CeRu_2Si_2$ with temperature. Since the Compton profile covers a wide range of momentum density (MD) distribution, it should reflect the overall picture of the electronic structure.

Within the framework of impulse approximation, the Compton profile, $J(p_z)$ is defined as $J(p_z) = \iint \rho(\mathbf{p}) dp_x dp_y$. Here, p_z is an electron momentum component in the direction of the scattering vector of x rays, and $\rho(\mathbf{p})$ denotes a MD. Since the Compton profile is described by the double integral of MD, the original MD distribution can be reconstructed from a number of Compton profiles measured in different crystal orientations. In addition, the application of the Lock-Crisp-West (LCW) analysis to the MD distribution gives an electron occupation number density (EOND) in k space which enables us to visualize the electronic structure in the first Brillouin zone (BZ) [22].

The sample measured was a single crystal of $CeRu_2Si_2$ grown by using the Czokralski pulling method in a triarc furnace. The T_K of the sample was evaluated to be 20 K from the result of magnetic susceptibility measurement. The HRCP measurements were made on the beam line BL08W at SPring-8, Japan. The energy of incident x ray was 115 keV, and the scattered x ray was energy resolved by a Ge(620) analyzer crystal and detected by a position sensitive detector. The momentum resolution was 0.11 atomic units (a.u.). Five directional HRCPs were measured at even intervals between the [100] and [110] crystal axes at 5 K and room temperature (RT). All the HRCPs were carefully corrected for the scattering cross section, background, multiple scattering, and x-ray absorption in the sample [23].

For comparison with experimental results, we have also carried out a band calculation on this system by using the local-density approximation based on the full-potential linearized augmented plane wave method, where the Ce-4f electron is treated as an itinerant one. The band structure obtained is consistent basically with the previously reported ones [15–19].

First we have compared the anisotropy of Compton profiles, which is the difference between Compton profiles measured in the [100] and [110] directions, with the theoretical one as shown in Fig. 1(a). Such subtraction eliminates the isotropic profiles of core electrons from the original profiles, and highlights the contribution of outer electrons. In the band calculation, the core electrons were treated as the one with isotropic MD distribution. The theoretical anisotropy is therefore reduced to almost zero in the region of more than 3 a.u., while experimental anisotropies slightly deviate from the theoretical one. This would indicate that the core electrons actually have a slightly anisotropic MD distribution. On the other hand, both measured and calculated anisotropies show a similar oscillatory structure. The oscillations are associated with characteristic distances corresponding to the coherence of wave functions in given crystal orientations [24,25]. Above T_K, the Ce-4f electron is well localized and regarded as a core state, while below T_K, the 4f electron forms a narrow conduction band where the 4f wave function has a shorter coherence length relative to the others. Such an aspect can

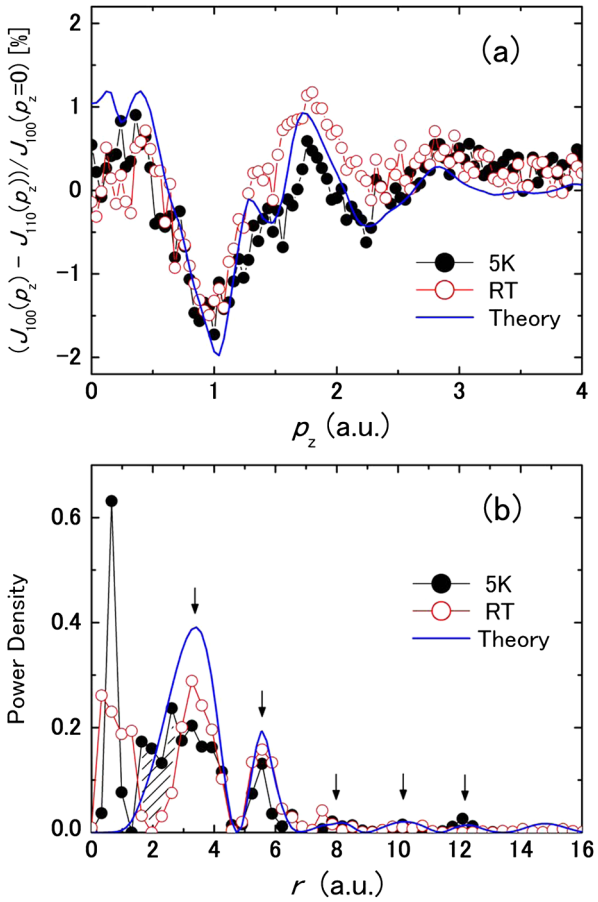

FIG. 1 (color online). Experimental and theoretical anisotropies of Compton profiles (a) which are shown in the percentage of the Compton peak measured in the [100] direction [24,25], and power densities (b) of the anisotropies. All the curves in (b) are normalized to a unit area [25]. In both figures, black solid and (red) open circles denote experimental ones at 5 K and RT, respectively. Solid (blue) lines are theoretical ones. The abscissas p_z and r are represented in atomic units.

be reflected in the power density, $|\int[J_{100}(p) - J_{110}(p)] \times \exp(-ipr)dp|^2$ as shown in Fig. 1(b). The intensities below 1 a.u. are probably attributed to the anisotropic MD distribution of core electrons as mentioned above. The peaks indicated by arrows correspond well to the theory, while the shaded area in the power density at 5 K shows a shift of spectral weight to shorter coherence length. Such a shift may arise from a lattice contraction at low temperatures. However, since the lattice contraction of the sample is less than 1% in the present temperature range, the effect of the lattice contraction on spectral shift can only go so far. The shift in Fig. 1(b) may suggest the formation of heavy fermions due to the hybridization of the 4f electron with the conduction electrons below T_K.

Next, the two-dimensional MD projected onto the (001) plane in momentum space was reconstructed from the HRCPs by the use of the direct Fourier transform method [26,27]. Then the LCW analysis, which folds the MD back

into the projected first BZ, was applied to the 2D MD to obtain 2D EOND. In the LCW procedure, the momentum densities of core electrons and fully occupied bands, in principle, make no contribution to the structure of EOND [22]. Therefore, the structure found in EOND reflects the electronic state of the itinerant electron. This aspect will allow us to observe the change from itinerant to localized electronic states. Actually, the structure of EOND may, however, be slightly distorted, because the LCW procedure is carried out within a finite momentum area; hence, the EOND of core electrons and fully occupied bands would show not the flat but spurious structure of some sort. We have, therefore, taken the following steps to eliminate the spurious structure from the original EOND. A mean profile was obtained from the average of the directional HRCPs and its smoothing. The reconstruction and LCW analyses were applied to the mean profile in a similar way. The mean EOND thus obtained was subtracted from the original EOND in the same momentum area. We verified that the resultant EOND showed a consistent structure regardless of folded momentum area, assuring a proper EOND of itinerant electron.

Figures 2(a) and 2(b), respectively, show 2D EONDs at 5 K and RT. It is clear that 2D EOND significantly changes around the corner of projected BZ; that is, a columnar structure observed at 5 K shrinks in size at RT. In the case of the 2D analysis, the densities at the X, W, and P points in the BZ are projected on the corner of 2D EOND, and the Z point is overlapped with the Γ point. The recent ARPES experiment has confirmed the difference of FS between $CeRu_2Si_2$ and $LaRu_2Si_2$ [5]. The noticeable difference appears along the direction connecting the X points in the BZ. The itinerant state of $CeRu_2Si_2$ shows a continuous tubular FS, whereas $LaRu_2Si_2$ has a discrete cigar-shaped FS along the vertical X-X direction. Such a difference in FS will appear as a change of intensity in 2D EOND. The structures in EOND are fundamentally formed only by conduction electrons from the viewpoint of the LCW prediction [22]. In addition, the integration of EOND corresponds to a FS volume. Therefore, the difference in size of the columnar structure between Figs. 2(a) and 2(b) indicate the change of the FS volume from the itinerant to the localized state, since the electronic state of $CeRu_2Si_2$ at

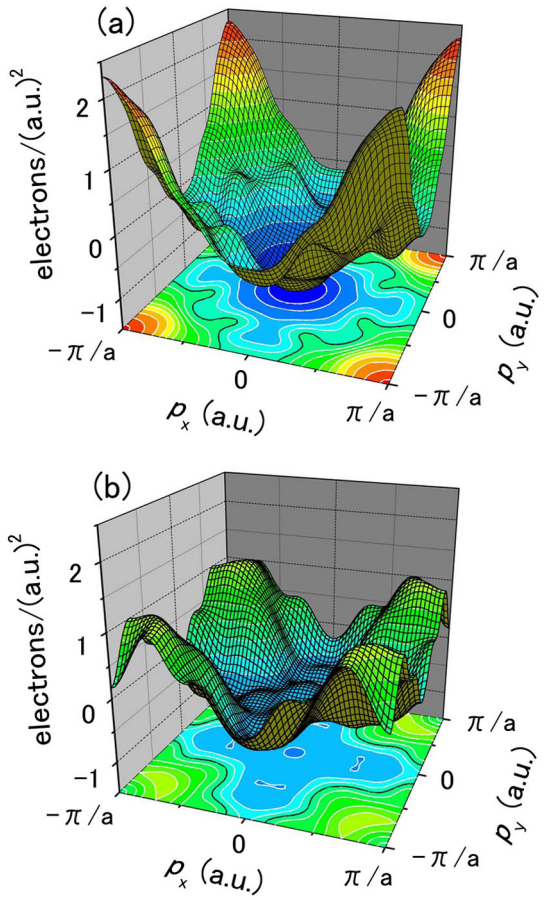

FIG. 2 (color online). 2D EONDs obtained at (a) 5 K and (b) RT.

temperatures far above T_K has been presumed to be the same as that of $LaRu_2Si_2$ with non-f electron. On the other hand, the ARPES measurement with resonance effect from Ce $3d$ to $4f$ states, which enhances the contribution of the $4f$ electron to the spectral intensity, has observed only a weak enhancement near the X point, while a remarkable enhancement has appeared around the Z point [5].

Then, we examined the contribution of the Ce-$4f$ electron to 2D EOND by contrast with the band calculation. Theoretical 2D EONDs have been derived from the wave functions of appropriate bands near the Fermi level. Figure 3 shows 2D EONDs of (a) the 14th, (b) the 15th,

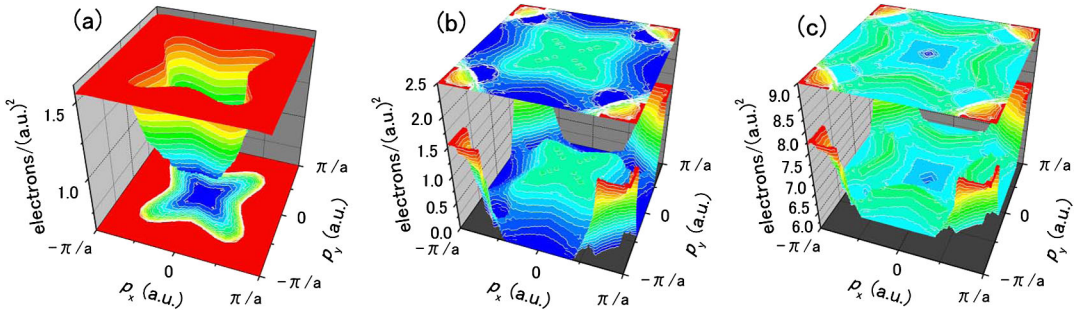

FIG. 3 (color online). Theoretical 2D EONDs of (a) the 14th, (b) the 15th, and (c) the sum total of relevant bands.

TABLE I. List of the electron occupation number of the Ce-f ($l = 3$) component at typical symmetric points in the 14th and 15th bands. The values are between 0 and 1.

	Γ	X	W	P	Z
14th Band	0.0000	0.2527	0.2204	0.0359	0.9677
15th Band	0.8827	0.9577	0.9544	0.9503	0.8725

and (c) the sum total of relevant bands. The depressed area in Fig. 3(a) reflects the hole contribution in the 14th band, while the pillar section at the corner in Fig. 3(b) is an indication of the electron contribution in the 15th band. It is obvious that the 14th and 15th bands account for a significant proportion of the total 2D EOND shown in Fig. 3(c). The theoretical 2D EOND in Fig. 3(c) reproduces the general appearance of the experimental one in Fig. 2(a) well, and the pillar section in Fig. 3(b) is consistent with the difference in density on the corner of the BZ between Figs. 2(a) and 2(b). Table I lists the electron occupation number of the Ce-f ($l = 3$) component at typical symmetric points in the 14th and 15th bands. The pillar section in Fig. 3(b) is found to be formed mainly by the projection of f electrons at the X, W, and P points in the 15th band on the corner of BZ. Therefore, the columnar structure in Fig. 2(a) is attributed to the Ce-4f electron in the 15th band, and the shrinkage of the columnar structure in Fig. 2(b) clearly specifies the localization of Ce-4f electron. In addition, it should be noted that the black lines in Fig. 2 indicate the zero line in the contour maps, that is, just about a border line between electron and hole contributions. The border line in Fig. 2(a) extends toward the corner of BZ. Its shape corresponds well to the hole FS observed around the Z point in the ARPES measurement with the resonance effect [5]. As shown in Fig. 3(a), the contours of the depressed area, which reflects the projected hole FS of the 14th band, show a X-shaped figure. Therefore, the difference of black lines between Figs. 2(a) and 2(b) indicates that the 14th band is also reconstructed along with the localization of the Ce-4f electron.

In conclusion, we have measured directional Compton profiles in the same $CeRu_2Si_2$ single crystal above and below T_K, and demonstrated the change of the electronic structure with the temperature from the aspect of 2D EOND. The most striking change of 2D EOND is observed around the corner of the projected BZ. The columnar structure appeared at 5K significantly contracts at RT. The difference in 2D EOND between 5K and RT is interpreted by contrast with the band calculation, and is attributed largely to the Ce $-$ 4f electrons in the 14th and 15th bands which change its nature from itinerant to localized ones. The Compton experiment is feasible without constraint on the experimental conditions such as temperature, magnetic field, pressure, and chemical substitution. Therefore, this technique will be also effective to systematically investigate the change of the electronic structure along with the metamagnetic transition in $CeRu_2Si_2$, the hidden order in URu_2Si_2, and other interesting phenomena of the heavy fermion system.

We are grateful to S. Teratani, T. Nagao, N. Yokoyama, H. Sakai, and M. Shiotsuki for their help with performing the Compton experiments. The synchrotron radiation experiments were performed with the approval of the Japan Synchrotron Radiation Research Institute (JASRI) (Proposal No. 2006B1463). This work was partially supported by a Grant-in-Aid for Scientific Research (No. 18340111) from the Ministry of Education, Culture, Sports, Science, and Technology (MEXT).

[1] P. Haen *et al.*, J. Low Temp. Phys. **67**, 391 (1987).
[2] P. Haen, H. Bioud, and T. Fukuhara, Physica B (Amsterdam) **259–261**, 85 (1999).
[3] M. Sugi *et al.*, Phys. Rev. Lett. **101**, 056401 (2008).
[4] P. Gegenwart, Q. Si, and F. Steglich, Nature Phys. **4**, 186 (2008).
[5] T. Okane *et al.*, Phys. Rev. Lett. **102**, 216401 (2009).
[6] G. J. Rozing *et al.*, Phys. Rev. B **43**, 9523 (1991).
[7] T. Ito *et al.*, Phys. Rev. B **60**, 13390 (1999).
[8] J. D. Denlinger *et al.*, J. Electron Spectrosc. Relat. Phenom. **117–118**, 347 (2001).
[9] A. F. Santander-Syro *et al.*, Nature Phys. **5**, 637 (2009).
[10] G. G. Lonzarich, J. Magn. Magn. Mater. **76–77**, 1 (1988).
[11] Y. Ōnuki *et al.*, J. Phys. Soc. Jpn. **61**, 960 (1992).
[12] H. Aoki *et al.*, Phys. Rev. Lett. **71**, 2110 (1993).
[13] F. S. Tautz *et al.*, Physica B (Amsterdam) **206–207**, 29 (1995).
[14] M. Takashita *et al.*, J. Phys. Soc. Jpn. **65**, 515 (1996).
[15] G. Zwicknagl, Phys. Scr. T **T49A**, 34 (1993).
[16] H. Yamagami and A. Hasegawa, J. Phys. Soc. Jpn. **62**, 592 (1993).
[17] E. K. R. Runge *et al.*, Phys. Rev. B **51**, 10375 (1995).
[18] M. A. Monge *et al.*, Phys. Rev. B **65**, 035114 (2002).
[19] M. Suzuki and H. Harima, J. Phys. Soc. Jpn. **79**, 024705 (2010).
[20] K. Miyake and H. Ikeda, J. Phys. Soc. Jpn. **75**, 033704 (2006).
[21] M. Yano *et al.*, Phys. Rev. B **77**, 035118 (2008).
[22] D. G. Lock, V. H. C. Crisp, and R. N. West, J. Phys. F **3**, 561 (1973). From the viewpoint of the LCW prediction, the electrons in localized orbitals and filled bands yield constant amplitude in EOND independently of wave number k because in such cases, every k point is occupied.
[23] N. Sakai, J. Phys. Soc. Jpn. **56**, 2477 (1987).
[24] A. Shukla *et al.*, Phys. Rev. B **59**, 12127 (1999).
[25] B. Barbiellini *et al.*, Phys. Rev. Lett. **102**, 206402 (2009).
[26] Y. Tanaka *et al.*, J. Phys. Chem. Solids **61**, 365 (2000).
[27] N. Hiraoka *et al.*, Phys. Rev. B **71**, 205106 (2005).